Density-functional theory investigation of electronic structure, elastic properties, optical properties, and lattice dynamics of Ba_2ZnWO_6*

Guo San-Dong(郭三栋)†

Department of Physics, School of Sciences, China University of Mining and Technology, Xuzhou 221116, *China*

(Received 11 September 2012; revised manuscript received 29 October 2012)

The electronic structures, optical dielectric functions, elastic properties, and lattice dynamics of Ba_2ZnWO_6 have been investigated by using the generalized gradient approximation. The density of states and distributions of charge density show that O and Ba tend toward ionic bond, but O and W or Zn display the covalent bond character. The calculated energy band structure shows that Ba_2ZnWO_6 is a wide indirect band gap semiconductor. The static value 2.28 of the refractive index is attained. The analysis of the elastic properties of Ba_2ZnWO_6 indicates a rather weak elastic anisotropy. The phonon dispersion is calculated, suggesting no structural instability, which is agreement with the recent low temperature neutron diffraction experiments. The mensurability C_v (phonon heat capacity) as the function of the temperature is also calculated to judge our results for future experiment.

Keywords: semiconductor, double perovskite structure, density-functional theory

PACS: 71.20.–b, 78.20.–e, 62.20.–x, 63.20.–e **DOI:** 10.1088/1674-1056/22/6/067102

1. Introduction

Due to their uncommon properties and potential applications, double perovskite A_2BCO_6 compounds have been investigated extensively.[1–10] The ideal double perovskite structure of the general formula A_2BCO_6 is constructed with the B cation substituted partially by a C cation in an ordered 1:1 way in the ideal perovskite structure ABO_3. Monoclinic, tetragonal, trigonal, and cubic structures have been discovered in this family,[11–15] some of which display this sequence on increase of temperature. For example, this compound of Ca_2MgWO_6 crystallizes in a monoclinic lattice, Sr_2MgWO_6 for a tetragonal lattice, Ba_2SrTeO_6 for a trigonal lattice, Ba_2MgWO_6 and Ba_2ZnWO_6 for a cubic lattice, and Sr_2MgWO_6 transforms to cubic lattice around 300 °C. The properties of this family of compounds under high pressure have also been researched. Structural evolutions of Sr_2MgWO_6 under high pressure have been carried out from angle dispersive X-ray diffraction and Raman scattering studies.[16] The high-pressure angle dispersive X-ray diffraction measurements up to 34.3 GPa for Ba_2MgWO_6 are studied, and it is found to be always stable for a cubic structure.[17] Recently, single crystals of the double perovskite structure Ba_2MgWO_6 and Ba_2ZnWO_6 have been grown for the first time with a cubic structure.[18] Related density function theory research has also been performed[19] for Ba_2MgWO_6.

Here, the generalized gradient approximation (GGA) within the density functional theory (DFT)[20,21] is used to investigate electronic structures, optical dielectric functions, elastic properties, and lattice dynamics of Ba_2ZnWO_6. The calculated crystal structures are in good agreement with experimental ones. The charge density shows the coexistence of an ionic bond character and a covalent bond character in the Ba_2ZnWO_6. The calculated static refractive index is 2.28. The non-dimensional anisotropy factor and the difference between the analytical maximum and minimum values of the Young's moduli show that Ba_2ZnWO_6 displays very weak anisotropy. The analysis of the lattice vibration shows that the Ba_2ZnWO_6 with a cubic structure is stable, which is in conformity with the low temperature experiment.[18] The phonon heat capacity has also been calculated, which can be used to confirm our results for future experiments.

The rest of the paper is organized as follows. In Section 2, we shall give our computational details. In Section 3, we shall present our main calculated results and analysis. Finally, we shall give our conclusion in Section 4.

2. Computational detail

We use a full-potential linearized augmented-plane-wave method within the DFT,[20,21] as implemented in the package WIEN2k.[22] The popular GGA by Wu Z, Cohen R (GGA-WC)[23] is used for the exchange–correlation potential to do our main DFT calculations. The full relativistic effects are calculated with the Dirac equations for core states, and the scalar relativistic approximation is used for valence states.[24–26] The spin–orbit coupling is neglected because it has little effect on our results. We use 1500 k points in the first Brillouin zone for the self-consistent calculation and 10000 k points for optical properties calculation, and make harmonic expansion up to $l_{max} = 10$ in each of the atomic spheres, and set $R_{mt} * k_{max} = 7$. The self-consistent calculations are considered

*Project supported by the Fundamental Research Funds for the Central Universities (Grant No. 2013QNA32).

†Corresponding author. E-mail: gsd@iphy.ac.cn

© 2013 Chinese Physical Society and IOP Publishing Ltd

to be converged when the integration of the absolute charge-density difference between the input and output electron density is less than $0.0001|e|$ per formula unit, where e is the electron charge. The phonon calculations are performed using the first principles package Quantum–ESPRESSO[27] using ultrasoft Perdew−Burke−Ernzerhof (PBE) pseudopotentials.[28] The kinetic energy cutoff is set for 35 Ry and a $8\times8\times8$ Monkhorst−Pack grid for the electronic Brillouin zone integration. By density functional perturbation theory (DFPT), a $4\times4\times4$ Monkhorst–Pack q–vector grid are calculated and the full phonon dispersion is obtained through Fourier interpolation.

3. Main results and analyses

3.1. Electronic structure

At first, the theoretical equilibrium crystal structure is obtained by means of total energy and force calculations, and the calculated lattice constant is 8.087 Å (1 Å = 0.1 nm), which is very close to the experimental value of 8.104 Å[18] obtained from neutron diffraction at 10 K. The theoretical O atomic position is (0.2387, 0, 0), which is also very close to the experimental value (0.2370, 0, 0) gained from the Rietveld refinement of the neutron diffraction data (298 K).[18]

The density of states (DOS) of Ba_2ZnWO_6 is shown in Fig. 1, including the total, the partial DOSs projected in Ba, Zn, W, and O atom spheres and the interstitial region. The Fermi level is set to be zero. The Ba valence band mainly covers from –10.7 eV to –9.5 eV, which distinctly separates from the O valence band between –6 eV and 0 eV. These show that O and Ba tend toward an ionic bond. The charge density distribution from the plane defined by O–Ba–O triangle perpendicular to (001) direction is used to illustrate this problem, which is presented in Fig. 2. The distributions of isoline of charge density near the Ba and O are both a whole string of ellipses, and they do not share the isoline directly, which indicates the ionic bond character between O and Ba. The Zn valence band forms strong hybridization with the O valence band near –5 eV, and the W valence band near –3.5 eV, which display the covalent bond character between Zn or W and O. The charge density distribution of the plane defined by a W–Zn–W triangle perpendicular to (001) direction is shown in Fig. 2. The Zn or W and O share the isoline of charge density directly, which shows that they tend toward the covalent bond character. From DOS, the O character band is mainly contributed to the bands near the Fermi energy level, and the bands near the bottom of conduction band are from the hybrid bands of W and O.

The energy band structure attained with GGA is present in Fig. 3. The calculated band gap is of an indirect character and equals to 2.99 eV, which is less than the reported experimental gap value of 3.5 eV. Since the energy gap is underestimated by the local density approximation (LDA) and GGA, a modified Becke–Johnson exchange plus local density approximation correlation potential (mBJLDA) was proposed recently by Tran and Blaha,[29] which can be used to produce accurate gaps for a wide range of different materials.[30–36] We also use mBJLDA to study the electronic structure of Ba_2ZnWO_6, and present the energy band in Fig. 3. The calculated gap with mBJLDA is 3.92 eV, which is improved by 0.93 eV than GGA. From energy bands, the mBJLDA changes valence bands little, and improves the conduction bands by 0.93 eV compared with GGA. However, the calculated gap with mBJLDA is larger than the experimental gap.

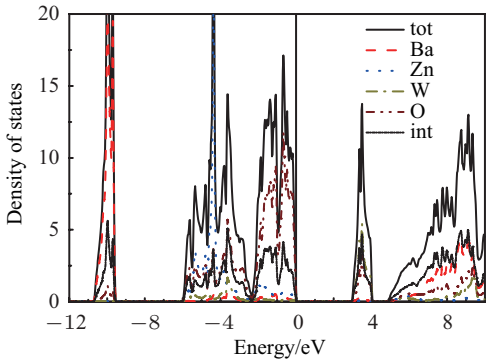


Fig. 1. (color online) The density of states of Ba_2ZnWO_6 calculated with GGA.

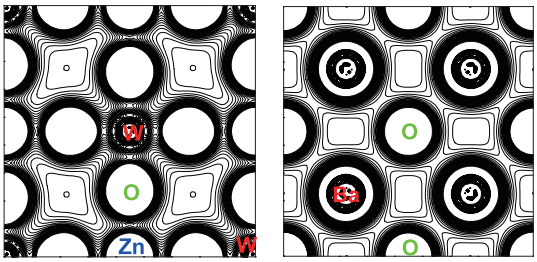


Fig. 2. (color online) The charge density distributions of Ba_2ZnWO_6, the planes are defined by W–Zn–W triangle (left) and O–Ba–O triangle (right) perpendicular to (001) direction: the actual charge density is 0.005–0.12 $|e|$/bohr^3 and the density increment is $0.005|e|$/bohr^3.

3.2. Optical properties

The frequency-dependent dynamic dielectric function is calculated after the electronic ground state has been obtained with GGA. Because the calculated gap is less than the experimental value, we use a scissors operator with 0.5 eV energy shift to match experimental gap. The frequency-dependent imaginary part of the dielectric function is determined by a hop summation from valence bands to conduction bands, and the real part of the dielectric tensor is obtained by the usual Kramers–Kronig transformation. The calculated dielectric function of Ba_2ZnWO_6 is shown in Fig. 4. There are two main peaks A and B below the low energy region in the imaginary part of dielectric function, and the first peak A is due to the the valence

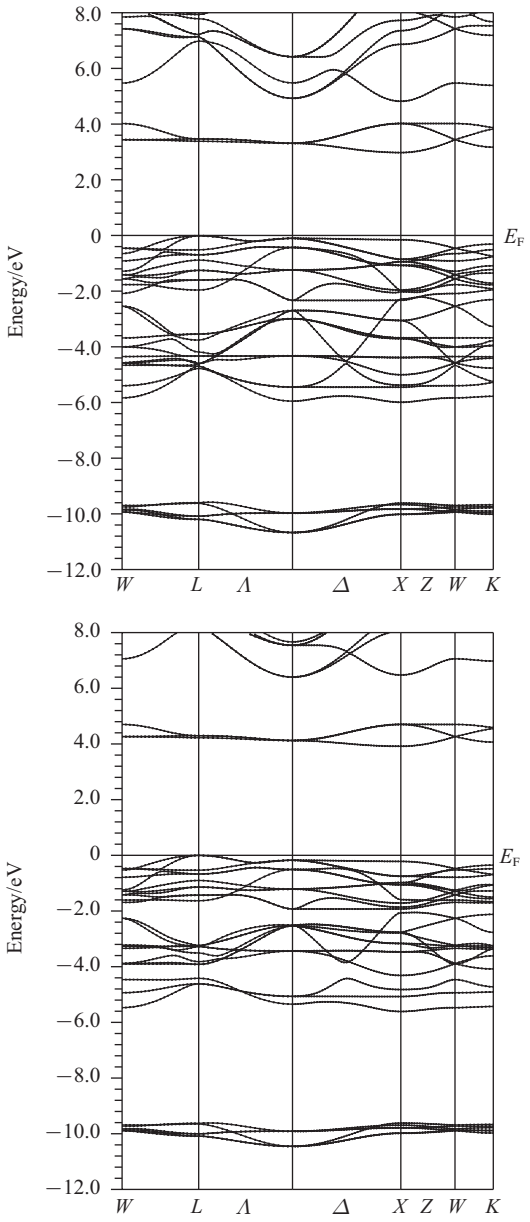


Fig. 3. The energy bands of Ba_2ZnWO_6 with GGA (top) and mBJLDA (bottom).

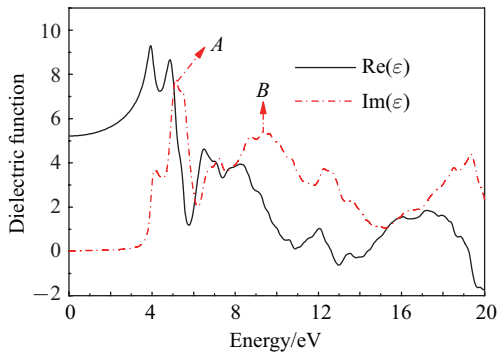


Fig. 4. (color online) The real and imaginary part of dielectric function of Ba_2ZnWO_6 calculated with GGA.

band—the first three conduction bands transitions, and the peak B from the valence band—the following conduction bands. The static value of the refractive index is 2.28 from a square root of its zero frequency real part of dielectric function 5.22.

3.3. Elastic constants

In this section, we present related elastic properties calculated with GGA similar to Ref. [19] for Ba_2MgWO_6. The elastic constants are a four-rank tensor. However, the elastic constants are reduced to three independent ones: C_{11}, C_{12}, C_{44} due to the symmetry for cubic crystal. The calculated values are $C_{11} = 320.70$, $C_{12} = 106.65$, $C_{44} = 103.24$ (unit: GPa) from the optimized structure. By applying the following mechanical stability criterion for the cubic materials, $C_{11} + 2C_{12} > 0$, $C_{44} > 0$, $C_{11} - C_{12} > 0$, the structural and mechanical stability of Ba_2ZnWO_6 is proved. The bulk modulus can be obtained by $B = (C_{11} + 2C_{12})/3$, and the value is 178.00 GPa, which is larger than 150.85 GPa for Ba_2MgWO_6. The anisotropy of the elastic properties can be measured by the so-called non-dimensional anisotropy factor A_G

$$A_G = \frac{G_V - G_R}{G_V + G_R}. \tag{1}$$

The G_V and G_R are upper (Voigt, G_V) and lower (Reuss, G_R) estimates of the shear moduli, for cubic materials by the following equations

$$G_V = \frac{C_{11} - C_{12} + 3C_{44}}{5}, \quad \frac{5}{G_R} = \frac{4}{C_{11} - C_{12}} + \frac{3}{C_{44}}. \tag{2}$$

The numerical calculations give the values $G_V = 104.75$ GPa, $G_R = 104.72$ GPa, and $A_G = 0.00016$ which is one magnitude smaller than 0.0045 for Ba_2MgWO_6. So small A_G indicates a very weak elastic anisotropy. The analytical maximum and minimum values of the Young's moduli are given in Ref. [37], and the numerical results are 267.47 GPa and 259.54 GPa for Ba_2ZnWO_6. The small difference shows clearly the rather weak elastic anisotropy again.

3.4. Lattice dynamics

In this section, we present the phonon spectra of Ba_2ZnWO_6 with the room temperature lattice constants of 8.121 Å.[18] Because the primitive unit cell contains ten atoms, the complete phonon spectrum consists of 30 dispersion curves: 3 acoustical and 27 optical ones. A group-theoretical analysis shows that the 27 zone-center optical modes are classified by the following symmetries: $T_{1g} + 4T_{1u} + 2T_{2g} + T_{2u} + E_g + A_{1g}$. The T_{1g}, T_{1u}, T_{2g}, and T_{2u} modes are triple-degenerate. The E_g mode is doubly-degenerate. Only the T_{1u} mode is infrared-active, while the T_{2g}, E_g, and A_{1g} modes are Raman-active.

Using DFPT, a $4 \times 4 \times 4$ Monkhorst–Pack q–vector grid was calculated and the full phonon dispersion was obtained through Fourier interpolation, which is presented in Fig. 5.

The calculated results show that no imaginary frequencies are produced, which implies the Ba_2ZnWO_6 with cubic structure is stable, and the low temperature neutron diffraction experiments revealed no structural phase transitions with a cubic phase.[18] However, the frequencies near the Γ point with T_{1g} modes is very low (20.15 cm^{-1} at the Γ point), and some of these family compounds undergo structure phase transitions, which is due to further softness of T_{1g} modes, such as Sr_2MgWO_6.[38] The T_{1g} modes originate from the vibration of O atoms only, and the T_{1g} mode instability can lead to a new structure with $R\bar{3}$ (148), $I4/m$ (87), $C2/m$ (12) or $P\bar{1}$ (2) symmetries by the group theory.[39] For example, the structure with $I4/m$ (87) symmetry is due to the rotation of the BO_6 octahedra around the fourfold axis, which is the room temperature structure for some of these family compounds, such as Sr_2MgWO_6.[38,40] To understand the distribution weight of the phonon energy, we also show the density of states in Fig. 5.

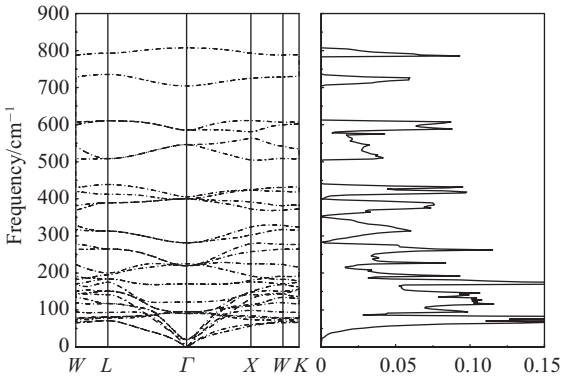


Fig. 5. The dispersion curves and density of states of phonon for Ba_2ZnWO_6 calculated with GGA.

The distribution of states is mainly focused between 0 cm^{-1} and 450 cm^{-1}. Within the quasiharmonic approximation, the phonon heat capacity C_v of Ba_2ZnWO_6 is also calculated, because the physical quantity can be measured directly from experiment, and the future experiments can judge our results. The phonon heat capacity as the function of the temperature is plotted in Fig. 6.

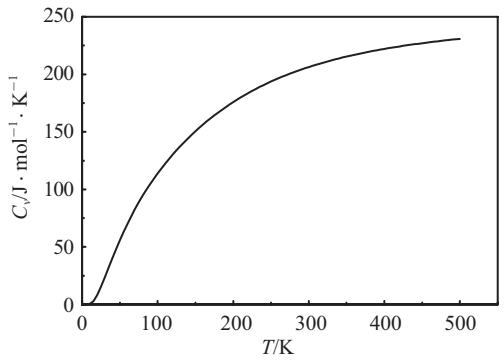


Fig. 6. Phonon heat capacity C_v of Ba_2ZnWO_6 calculated with GGA.

4. Conclusion

In summary, we have used a state-of-the-art DFT method to investigate the electronic structures, elastic properties, optical properties, and lattice dynamics of Ba_2ZnWO_6. The related data are summarized in Table 1. The calculated crystal structure with GGA-WC are very close to experimental one from neutron diffraction. The O and Ba tend toward an ionic bond, but O and W or Zn display the covalent bond character, which can been shown by the density of states and distributions of charge density. The Ba_2ZnWO_6 is a wide indirect band gap semiconductor, the gap is 2.99 eV calculated with GGA and 3.92 eV with mBJLDA, however, the experimental one is 3.5 eV. The analyses of the elastic properties show that the elastic anisotropy of Ba_2ZnWO_6 is rather weak, and the bulk modulus B and the analytical minimum and maximum values of the Young's moduli Y_{min}, Y_{max} are also calculated under the pressure 178 GPa, 259.54 GPa, and 267.47 GPa, respectively. The frequency-dependent dynamic dielectric function has been calculated, and the zero-frequency refractive index $n(0)$ has also been attained to be 2.28. The structural stability is proved by the phonon calculation, which is agreement with the recent low temperature neutron diffraction experiments. The thermodynamic quantities C_v (phonon heat capacity) have been calculated within the quasiharmonic approximation as further experimental judgment.

Table 1. The lattice constants a and the internal atomic parameters u_x with GGA (experiment); the gaps obtained with GGA[mBJLDA] (experiment); the zero-frequency refractive index $n(0)$; the bulk modulus B, and the analytical minimum and maximum values of the Young's moduli Y_{min}, Y_{max}; the frequency for T_{1g} mode.

a/Å	u_x	Gap/eV	$n(0)$
8.087 (8.104)	0.2387 (0.2370)	2.99[3.92] (3.5)	2.28
B/GPa	Y_{min}/GPa	Y_{max}/GPa	T_{1g}/cm^{-1}
178	259.54	267.47	20.15

References

[1] Kobayashi K I, Kimura T, Sawada H, Terakura K and Tokura Y 1998 *Nature* **395** 677
[2] Kobayashi K I, Kimura T, Tomioka Y, Sawada H, Terakura K and Tokura Y 1999 *Phys. Rev. B* **59** 11159
[3] Tomioka Y, Okuda T, Okimoto Y, Kumai R, Kobayashi K I and Tokura Y 2000 *Phys. Rev. B* **61** 422
[4] Rogado N S, Li J, Sleight A W and Subramanian M A 2005 *Adv. Mater.* **17** 2225
[5] Lee K W and Pickett W E 2008 *Phys. Rev. B* **77** 115101
[6] Wu H P, Qian Y and Lu R F 2011 *Appl. Phys. Lett.* **99** 123116
[7] Shan Y J, Ozeki A, Luan W, Nakamura T and Itoh M 2001 *Ferroelectrics* **264** 175
[8] Wu H P, Lu R F, Tan W S, Xiao C Y, Deng K M and Qian Y 2012 *Appl. Phys. Lett.* **100** 132404
[9] Zhou W L, Zhang Q L, Gao J Y, Liu W P, Ding L H and Yin S T 2011 *Chin. Phys. B* **20** 016101
[10] Wang J H, Yu Z, Liu G Q and Du Y W 2004 *Chin. Phys.* **13** 90
[11] Gateshki M, Igartua J M and Hernandez-Bocanegra E 2003 *J. Phys.: Condens. Matter* **15** 6199
[12] Gateshki M and Igartua J M 2003 *J. Phys.: Condens. Matter* **15** 6749

[13] Fu W T, Au Y S, Akerboom S and Ijdo D J W 2008 *J. Solid State Chem.* **181** 2523
[14] Patwe S J, Achary S N, Mathews M D and Tyagi A K 2006 *Mater. Chem. Phys.* **98** 486
[15] Patwe S J, Achary S N, Mathews M D and Tyagi A K 2005 *J. Alloys Compd.* **390** 100
[16] Mishra A K, Poswal H K, Acharya S N, Tyagi A K and Sharma S M 2010 *Phys. Status Solidi B* **247** 1773
[17] Meenakshi S, Vijayakumar V, Achary S N and Tyagi A K 2011 *J. Phys. Chem. Solids* **72** 609
[18] Bugaris Daniel E, Hodges Jason P, Ashfia Huq and Hans-Conrad zur Loye 2011 *J. Solid State Chem.* **184** 2293
[19] Brik M G 2012 *J. Phys. Chem. Solids* **73** 252
[20] Hohenberg P and Kohn W 1964 *Phys. Rev.* **136** B864
[21] Kohn W and Sham L J 1965 *Phys. Rev.* **140** A1133
[22] Blaha P, Schwarz K, Madsen G K H, Kvasnicka D and Luitz J 2001 WIEN2k, an Augmented Plane Wave + Local Orbitals Program for Calculating Crystal Properties (Karlheinz Schwarz Technische University at Wien, Austria) ISBN 3-9501031-1-2
[23] Wu Z G and Cohen R E 2006 *Phys. Rev. B* **73** 235116
[24] MacDonald A H, Pickett W E and Koelling D D 1980 *J. Phys. C* **13** 2675
[25] Singh D J and Nordstrom L 2006 *Plane Waves, Pseudopotentials and the LAPW Method*, 2nd edn. (New York: Springer)
[26] Kunes J, Novak P, Schmid R, Blaha P and Schwarz K 2001 *Phys. Rev. B* **64** 153102
[27] Giannozzi P, Baroni S, Bonini N, *et al.* 2009 *J. Phys. : Condens. Matter* **21** 395502
[28] Perdew J P, Burke K and Ernzerhof M 1996 *Phys. Rev. Lett.* **77** 3865
[29] Tran F and Blaha P 2009 *Phys. Rev. Lett.* **102** 226401
[30] Singh D J 2010 *Phys. Rev. B* **82** 205102
[31] Guo S D and Liu B G 2011 *J. Appl. Phys.* **110** 073525
[32] Guo S D and Liu B G 2011 *Europhys. Lett.* **93** 47006
[33] Singh D J 2010 *Phys. Rev. B* **82** 155145
[34] Singh D J, Seo S S A and Lee H N 2010 *Phys. Rev. B* **82** 180103
[35] Guo S D and Liu B G 2012 *J. Phys.: Condens. Matter* **24** 045502
[36] Guo S D and Liu B G 2012 *Chin. Phys. B* **21** 017101
[37] Cazzani A and Rovati M 2003 *Int. J. Solids Struct.* **40** 1713
[38] Guo S D and Liu B G 2013 *Physica B: Condens. Matter.* **408** 110
[39] Stokes H T, Hatch D M and Campbell B J 2007 ISOTROPY, stokes.byu.edu/isotropy.html.
[40] Gateshki M and Igartua J M 2004 *J. Phys.: Condens. Matter* **16** 6639